HHS Public Access

Author manuscript

Neuroimage. Author manuscript; available in PMC 2016 April 15.

Published in final edited form as:

Neuroimage. 2015 April 15; 110: 162–170. doi:10.1016/j.neuroimage.2015.01.041.

Central Artery Stiffness, Baroreflex Sensitivity, and Brain White Matter Neuronal Fiber Integrity in Older Adults

Takashi Tarumi[a,b], **Daan L.K. de Jong**[c], **David C. Zhu**[d], **Benjamin Y. Tseng**[a,b], **Jie Liu**[a,b], **Candace Hill**[a], **Jonathan Riley**[a], **Kyle B. Womack**[e,f], **Diana R. Kerwin**[g], **Hanzhang Lu**[h], **C. Munro Cullum**[e,f], and **Rong Zhang**[a,b,f]

[a]Institute for Exercise and Environmental Medicine, Texas Health Presbyterian Hospital Dallas (8200 Walnut Hill Ln, Dallas, TX, USA 75231) [b]Department of Internal Medicine, University of Texas Southwestern Medical Center (1801 Inwood Rd, Dallas, TX, USA 75235) [c]Department of Geriatric Medicine, Radboud University Medical Center (Geert Grooteplein-Zuid 10, 6525 GA Nijmegen, Netherlands) [d]Department of Radiology and Psychology, and Cognitive Imaging Research Center, Michigan State University (220 Trowbridge Rd, East Lansing, MI, USA 48824) [e]Department of Psychiatry, University of Texas Southwestern Medical Center (1801 Inwood Rd, Dallas, TX, USA 75235) [f]Department of Neurology and Neurotherapeutics, University of Texas Southwestern Medical Center (1801 Inwood Rd, Dallas, TX, USA 75235) [g]Texas Alzheimer's and Memory Disorders, Texas Health Presbyterian Hospital Dallas (8200 Walnut Hill Ln, Dallas, TX, USA 75231) [h]Advanced Imaging Research Center, University of Texas Southwestern Medical Center (1801 Inwood Rd, Dallas, TX, USA 75235)

Abstract

Cerebral hypoperfusion elevates the risk of brain white matter (WM) lesions and cognitive impairment. Central artery stiffness impairs baroreflex, which controls systemic arterial perfusion, and may deteriorate neuronal fiber integrity of brain WM. The purpose of this study was to examine the associations among brain WM neuronal fiber integrity, baroreflex sensitivity (BRS), and central artery stiffness in older adults. Fifty-four adults (65±6 years) with normal cognitive function or mild cognitive impairment (MCI) were tested. The neuronal fiber integrity of brain WM was assessed from diffusion metrics acquired by diffusion tensor imaging. BRS was measured in response to acute changes in blood pressure induced by bolus injections of vasoactive drugs. Central artery stiffness was measured by carotid-femoral pulse wave velocity (cfPWV). The WM diffusion metrics including fractional anisotropy (FA) and radial (RD) and axial (AD) diffusivities, BRS, and cfPWV were not different between the control and MCI groups. Thus, the

Corresponding Author: Rong Zhang, Ph.D. Institute for Exercise and Environmental Medicine Texas Health Presbyterian Hospital Dallas University of Texas Southwestern Medical Center Address: 7232 Greenville Ave, Dallas, TX 75231 Telephone: (214) 345-8843 Fax: (214) 345-4618 rongzhang@texashealth.org.

Conflict of Interest None

data from both groups were combined for subsequent analyses. Across WM, fiber tracts with decreased FA and increased RD were associated with lower BRS and higher cfPWV, with many of the areas presenting spatial overlap. In particular, the BRS assessed during hypotension was strongly correlated with FA and RD when compared with hypertension. Executive function performance was associated with FA and RD in the areas that correlated with cfPWV and BRS. These findings suggest that baroreflex-mediated control of systemic arterial perfusion, especially during hypotension, may play a crucial role in maintaining neuronal fiber integrity of brain WM in older adults.

Keywords

Arterial stiffness; baroreflex sensitivity; neuronal fiber integrity; cognitive function; mild cognitive impairment

Introduction

Cardiovascular aging and disease are associated with an elevated risk for structural and functional abnormalities in the brain (Kivipelto et al., 2001; Rusanen et al., 2014). In particular, white matter (WM) lesions, a strong risk factor for cognitive impairment, have consistently been shown to correlate with central artery stiffness (Longstreth et al., 1996; Tsao et al., 2013). WM lesions may develop from hypoperfusion and/or ischemia (Fernando et al., 2006; Moody et al., 1990). Under normal conditions, arterial perfusion pressure, especially those of short-term variability in seconds and minutes, is controlled by arterial baroreflex (Koepchen, 1984). Arterial baroreceptors, a type of mechanoreceptor located in the central elastic arteries, monitor changes in transmural pressure via the vessel wall distortion (Lanfranchi and Somers, 2002). With age and/or presence of cardiovascular disease risk factors, a reduction in central arterial compliance attenuates baroreflex sensitivity for a given change in blood pressure (Monahan et al., 2001; Tanaka et al., 2000). As a result, the depressed baroreflex sensitivity (BRS) may impair cardiovascular regulation of systemic arterial perfusion (Rothwell, 2010; Rothwell et al., 2010). To date, there have been no studies investigating the relation between brain WM structural integrity and BRS.

Diffusion tensor imaging (DTI) can quantitatively assess microstructural changes in WM neuronal fiber tracts that manifest with aging or neurodegenerative disease (de Groot et al., 2013; Maillard et al., 2014). Measuring the anisotropic property of water molecule diffusions in a WM fiber tract, DTI provides several key metrics, including fractional anisotropy (FA) and radial and axial diffusivities (RD and AD respectively) (Mori and Zhang, 2006). FA reflects WM neuronal fiber integrity that is determined by density, directional coherence, and myelination level of WM fibers (Beaulieu and Allen, 1994). RD and AD further provide structural information about WM neuronal fibers. Histological studies suggested that higher RD indicates axonal demyelination, while lower AD reflects axonal loss (Song et al., 2003). Importantly, alterations in these diffusion metrics correlate with neurocognitive performance, especially executive function (Madden et al., 2009).

Dementia manifests at the end of a pathological spectrum, extending from age-related cognitive decline and functional impairment (Jack Jr et al., 2013; Wentzel et al., 2001). Mild

cognitive impairment (MCI) represents an intermediate disease stage which may be a suitable target to alter the pathological trajectory via life-style and/or pharmacological interventions (Gauthier et al., 2006). Therefore, physiological understanding of the mechanisms linking cardiovascular and cognitive health in MCI is crucial. The main aim of the present study was to determine the impact of central artery stiffness and BRS on WM neuronal fiber integrity in older adults with or without MCI. Specifically, we hypothesized that: 1) central artery stiffness and depressed BRS would be associated with the lower levels of WM neuronal fiber integrity as assessed by DTI, and these abnormalities are exacerbated in MCI when compared with normal older adults, and 2) executive function performance would be associated with WM neuronal fiber integrity in the area(s) that correlates with central artery stiffness and BRS.

Materials and Methods

Study Participants

Fifty-four participants (18 cognitively normal and 36 MCI subjects) were recruited through a community-based advertisement using local newspapers, senior centers, and the University of Texas Southwestern Medical Center Alzheimer's Disease Center. The diagnosis of MCI was based on the Petersen criteria (Petersen et al., 2001; Petersen et al., 1999), as modified by the Alzheimer's Disease Neuroimaging Initiative project (http://adni-info.org). Clinical evaluation was performed based on the recommendations from Alzheimer's Disease Cooperative Study (http://adni-info.org). Inclusion criteria were men and women aged 55-80 years who were diagnosed with MCI or judged to be cognitively normal. Exclusion criteria included major psychiatric disorders, major or unstable medical conditions, uncontrolled hypertension, diabetes mellitus, current or a history of smoking within the past 2 years, or chronic inflammatory diseases. Individuals with a pacemaker or any metal in their body which precluded magnetic resonance imaging were excluded. Subjects engaging in regular aerobic exercise in the past 2 years were excluded because physical activity may alter brain structure and function, independently of vascular disease and risk factors (Cotman et al., 2007). All subjects signed the informed consent approved by the Institutional Review Boards of University of Texas Southwestern Medical Center and Texas Health Presbyterian Hospital of Dallas.

Measurements

Magnetic Resonance Imaging (MRI)—All MRI measurements were acquired by a 3-Tesla scanner (Philips Medical System, Best, The Netherlands) using a body coil for radiofrequency transmission and 8-channel head coil with parallel imaging capability for signal reception. Three MRI sequences were performed: DTI, fluid-attenuated-inversion-recovery (FLAIR), and 3D magnetization-prepared rapid acquisition gradient echo (MPRAGE). DTI was acquired using a single-shot echo-planar-imaging (EPI) sequence with a sensitivity encoding (SENSE) parallel imaging scheme (reduction factor=2.2). The imaging matrix was 112×112 with field of view (FOV) =224×224 mm^2 (nominal resolution of 2 mm), which was filled to 256×256. Axial slices of 2.2 mm thickness (no gap) were acquired parallel to the anterior-posterior commissure line. A total of 65 slices covered the entire hemisphere and brainstem. Echo Time (TE)/Repetition Time (TR) was 51/5630 ms.

The diffusion weighing was encoded along 30 independent orientations and the b value was 1000 s/mm^2. The scan duration was 4.3 minutes. Automated image registration was performed on the raw diffusion images to correct distortions caused by motion artifacts or eddy currents. All subjects underwent two consecutive scans of DTI acquisitions.

FLAIR images were acquired in the transverse plane using the following parameters: FOV=230×230 mm^2, resolution=0.65 (anterior-posterior) ×0.87 (right-left) mm^2, number of slices=24, thickness=5 mm, gap=1 mm, TR/Inversion Time/TE=11000/2800/150 ms, and scan duration=3.6 minutes. MPRAGE images were acquired using the following parameters: TE/TR=3.7/8.1 ms, flip angle=12°, FOV=256×256 mm, number of slices = 160 (no gap), resolution=1×1×1 mm^3, SENSE factor=2, and scan duration=4 minutes.

Cardiovascular Assessments—All physiological measurements were performed in an environmentally controlled laboratory after resting in the supine position for ≥15 minutes. All subjects abstained from alcohol, caffeinated beverages, and intense physical activity for ≥12 hours prior to data collection. Brachial blood pressure was measured intermittently using an electrosphygmomanometer (Suntech, Morrisville, NC, USA). Central artery stiffness was measured by carotid-femoral pulse wave velocity (cfPWV) using applanation tonometry which was sequentially placed on the common carotid and femoral arteries (SphygmoCor 8.0; AtCor Medical, West Ryde, NSW, Australia). Arterial pulse of >10 cardiac cycles was recorded to calculate cfPWV.

BRS was assessed via the modified Oxford protocol in which we performed a sequential intravenous bolus injections of sodium nitroprusside (100 μg) followed 60 seconds by phenylephrine hydrochloride (150 μg). All subjects experienced a decrease and increase in systolic blood pressure of at least 15 mmHg. Three-lead electrocardiogram (ECG) and beat-by-beat arterial blood pressure using finger plethysmography (Finapress; Ohmeda, Boulder, CO, USA) were continuously recorded with a sampling frequency of 1,000 Hz and analyzed offline using data analysis software (Acqknowledge, BIOPAC Systems, Goleta, CA, USA).

Neurocognitive Assessments—Clinical Dementia Rating (CDR) (Morris et al., 1997), Mini-mental State Examination (MMSE) (Folstein et al., 1975), Wechsler Memory Scale-Revised (WMS-R) (Wechsler, 1987), California Verbal Learning Test-second edition (CVLT-II) (Delis, 2000), and Trail Making Test parts A and B (Tombaugh, 2004) were administered and scored using standard criteria. The diagnosis of MCI was determined by a global CDR of 0.5 with a score of 0.5 in the memory category, objective memory loss as indicated by education-adjusted scores on the Logical Memory subtest of the WMS-R, and MMSE score between 24 and 30. CVLT-II Long Delay Free Recall and Trail Making Test part B minus A (i.e., to focus more upon the executive function components of the test by subtracting the psychomotor speed aspect) were selected *a priori* as the primary measures of memory and executive function, respectively (Drane et al., 2002; Grundman et al., 2004).

Data Analyses

DTI Preprocessing and Analysis—DTI data were preprocessed using the FMRIB Diffusion Toolbox (FDT) included as a part of the FMRIB Software Library (FSL) program (http://www.fmrib.ox.ac.uk/fsl, Oxford Center for Functional MRI of the Brain, Oxford

University, UK) (version 5.0). First, 2 scans of DTI data were merged in the temporal order, corrected for eddy currents and head motion, and averaged over the scans to increase signal-to-noise ratio. Second, a brain mask was created using Brain Extraction Tool (BET). Finally, the diffusion tensor was calculated by fitting a diffusion tensor model to the preprocessed DTI data using the DTIfit program included in FDT (Smith, 2002). To minimize partial volume effects from grey matter and cerebrospinal fluid, we set a threshold for voxels with FA value greater than 0.20. Individual subjects' images with FA, RD, and AD were visually inspected and used in the voxelwise and region-of-interest (ROI) analyses.

Voxelwise statistics were performed by tract-based spatial statistics (TBSS) (version 1.2) (Smith et al., 2006), a part of the FSL program (Smith et al., 2004). All subjects' FA data were first aligned into a common space using the FMRIB's nonlinear image registration tool (FNIRT), which uses a b-spline representation of the registration warp field (Rueckert et al., 1999). We used *JHU-ICBM-FA* template as a common space in order to correspond the results from voxelwise and ROI analyses. Next, the mean FA image was created and thinned to generate a mean FA skeleton which represents the centers of all tracts common to all subjects. Each subject's aligned FA, RD, and AD data were projected onto this skeleton and the resulting data were fed into voxelwise and ROI-based cross-subject statistics.

ROI analysis that is limited to the TBSS skeleton was performed using the deep WM atlas (*ICBM-DTI-81 white-matter atlas*) developed by the Johns Hopkins University (Mori et al., 2008). Mean values of a diffusion metric for selected ROI segmentations were extracted from each participant.

WM Lesion Volume—Total brain volume of WM hyperintensities were measured in FLAIR images using a procedure described in detail elsewhere (Gurol et al., 2006). First, a ROI corresponding to WM hyperintensity was created using a semi-automated technique which applies individually determined intensity thresholding. Second, gross manual outlining of WM hyperintensities was performed to create ROI maps. Third, the intersection of ROIs created from the 1st and 2nd steps were identified, visually inspected, and produced the final WM hyperintensity volume. To account for individual differences in head size, total brain volume of WM hyperintensity was normalized to the intracranial volume and reported in percentage. *Baroreflex Sensitivity*. Cardiovagal BRS was analyzed using the procedure described in detail elsewhere (Lipman et al., 2003; Rudas et al., 1999). Briefly, individual raw data showing the relation between R-R interval and systolic blood pressure was first plotted to visually identify and exclude the saturation and threshold regions. Next, the values of R-R interval were pooled and averaged every 2 mmHg bin of systolic blood pressure to minimize the influence of respiration. A least squares linear regression was applied to the relation between changes in systolic blood pressure and R-R interval of the preceding cardiac cycle to account for baroreflex delays. BRS was determined by a slope of the linear regression, with a correlation coefficient greater than 0.80. BRS was calculated from the entire sequence of the modified Oxford protocol as well as hypo- and hypertensive episodes separately.

Central Artery Stiffness—Carotid-femoral PWV was calculated by dividing arterial pulse traveling distance by the transit time, and expressed in meters per second. The

traveling distance was measured as a straight distance on body surface between the carotid and femoral arteries using a tape ruler. The arterial pulse transit time was calculated by subtracting a time difference between the R-wave of ECG to a foot of femoral artery pressure waveform minus a time difference between the R-wave of ECG to a foot of carotid artery pressure waveform. The transit time was averaged over >10 cardiac cycles.

Brain Volume—Global and regional brain volumes were measured using FreeSurfer software (https://surfer.nmr.mgh.harvard.edu/fswiki). Global brain volume (i.e., total parenchyma, and grey and white matters) was normalized to intracranial volume whereas regional brain volume (i.e., medial temporal lobe and hippocampus) was corrected for total parenchyma volume in order to estimate regional tissue loss, independent of the global effect (Wardlaw et al., 2013).

Statistical Analysis

All participants completed the study protocol. Voxelwise analysis of DTI data was performed by general linear model, a part of the FSL-randomise program. Diffusion metrics were first compared between the groups of normal and MCI subjects. Then, the associations with cfPWV and BRS were examined. To further explore the impact of hypo- and hypertension on the brain structure, we performed an additional TBSS analysis using BRS to separately assess the effects of blood pressure reduction and elevation. Correction for multiple comparisons was performed using threshold-free cluster enhancement (TFCE) with 5,000 permutations. Corrected statistical maps were further thresholded by $P<0.05$. Anatomical assignments of the WM skeleton voxels that survived correction of multiple comparisons and P-value thresholding were identified using the WM atlas. We specifically focused on the major WM fiber tracts in the deep and periventricular area which may be susceptible for cerebral hypoperfusion and/or ischemia (Moody et al., 1990). These WM fiber tracts included corpus callosum, corona radiate, internal capsule, external capsule, and superior longitudinal fasciculus. Finally, the mean values of diffusion metrics were extracted from the significant WM skeletons resulting from the TBSS analysis.

The groups of normal and MCI subjects were compared by the Mann-Whitney *U* test. Simple correlations among continuous variables were examined by the Pearson's product-moment correlation. Multiple linear regression was used to examine the association of diffusion metrics with cfPWV and BRS, including covariates. All models adjusted for age, sex, education level, systolic blood pressure, and correlates of cfPWV, BRS, and diffusion metrics in this sample. Partial correlation was used to test the association between diffusion metrics and cognitive function. The covariates included in this analysis were age, sex, education level, systolic blood pressure, and correlates of cognitive function in this sample.

Normality of continuous variables was examined by the Shapiro-Wilk test as well as the visual inspection of histograms and Q-Q plots. Total brain volume of WM hyperintensity was log-transformed due to a skewed distribution of the raw data. Sex was dummy-coded (men=0 and women=1). Statistical significance was set *a priori* at $P<0.05$ for all tests. Data are reported as mean ± standard deviation. Statistical analyses were performed using SPSS 21.0 (SPSS inc., Chicago, IL).

Results

Table 1 shows a group comparison of the normal and MCI subjects. Age, sex, education level, and MMSE scores did not differ between groups. Compared with the normal group, MCI subjects demonstrated lower performance in memory and executive function, as evidenced by the lower scores on CVLT-II Long Delay Free Recall and the longer time in Trail Making Test B-A respectively. In contrast, there was no group difference in the measures of diffusion metrics, brain volume, and cardiovascular function including cfPWV and BRS. Accordingly, all subjects' data were combined to perform the association analyses.

Consistent with the literatures (Monahan et al., 2001; Tanaka et al., 2000), higher cfPWV correlated with lower BRS ($r=-0.34$, $P=0.01$), assessed particularly during hypotension ($r=-0.45$, $P=0.001$) compared with hypertension ($r=-0.26$, $P=0.06$). The greater volume of WM hyperintensity correlated with lower BRS ($r=-0.35$, $P=0.01$) and higher cfPWV ($r=0.68$, $P<0.001$).

Associations among central artery stiffness, BRS, and WM neuronal fiber integrity

In Figure 1, TBSS maps exhibit WM fiber tracts that associated with cfPWV and BRS. Specifically, 46.6 cm^3 and 43.1 cm^3 of the WM fiber tracts with decreasing FA were associated with higher cfPWV and lower BRS, respectively. Similarly, 48.8 cm^3 and 31.9 cm^3 of the WM fiber tracts with increasing RD were associated with higher cfPWV and lower BRS, respectively. When BRS was analyzed separately during hypo- and hypertension, the former was associated with the greater volume of WM fiber tracts with FA (43.0 vs. 21.8 cm^3) and RD (36.0 vs. 0.08 cm^3) when compared with the latter, while the directions of associations remained the same as the combined BRS (Figure 2). WM fiber tracts with AD did not correlate with either cfPWV or BRS.

The WM fiber tracts that associated with cfPWV and BRS exhibited a large spatial overlap. Specifically, 25.0 cm^3 and 21.6 cm^3 of the voxels with FA and RD were associated with both cfPWV and BRS, respectively (bottom of the Figure 1). This accounts for ~50% of the WM fiber tracts that correlated with either cfPWV or BRS, and may suggest the presence of a common underlying mechanism by which central artery stiffness and low BRS deteriorate WM neuronal fiber integrity or they may contribute independently to the neuronal fiber deterioration in these regions. To explore these possibilities, we extracted the mean values of individual FA and RD from the spatial overlapped regions and further examined their associations with cfPWV and BRS. Figure 3 shows the scatter plots of cfPWV and BRS in relation to FA and RD extracted from the global WM skeletons. Multivariate adjusted regression revealed significant associations of the global WM skeletons with cfPWV and BRS after controlling for age, sex, education level, systolic blood pressure, and WM hyperintensity volume (Tables 2 and 3).

Similar to the global WM analysis, many of the WM fiber tracts in the deep and periventricular area showed spatial overlap in terms of their associations with cfPWV and BRS. Multivariate adjusted regression revealed that both cfPWV and BRS independently associated with FA and RD in the posterior corona radiata (PCR) (Tables 2 and 3). In

addition, BRS independently associated with FA and RD in the splenium of corpus callosum and the retrolenticular part of internal capsule.

Association between WM neuronal fiber integrity and cognitive function

Better executive function performance, as assessed by Trail Making Test B-A, was associated with the higher levels of FA and the lower levels of RD in the global WM skeletons that correlated with both cfPWV and BRS (Figure 4). Partial correlation analysis further revealed that FA and RD measured from the global WM ($r=-0.32$ with $P=0.03$; $r=0.31$ with $P=0.04$, respectively) and RD measured from the PCR ($r=0.29$ with $P=0.048$) remain to be correlated with executive function performance after controlling for age, sex, education level, systolic blood pressure, WM hyperintensity volume, and cognitive status (i.e., healthy or MCI group).

Discussion

The major findings from this study are as follows. First, central artery stiffness and depressed BRS were independently associated with the deterioration of WM neuronal fiber integrity, as reflected by the decreases in FA and increases in RD. In addition, a large portion of the WM fiber tracts with FA and RD that correlated with arterial stiffness and BRS showed spatial overlap. Second, WM neuronal fiber integrity was correlated more strongly with BRS assessed during hypotension than hypertension. Third, executive function performance was associated with WM neuronal fiber integrity, specifically in the areas correlated with arterial stiffness and low BRS. Below we further discuss the potential mechanism(s) and clinical implications of these findings.

The role of baroreflex in the link between central artery stiffness and WM neuronal fiber integrity

Central artery stiffness was associated with abnormal structural changes in the brain WM, as assessed by both WM hyperintensity and DTI. The cross-sectional association between aortic PWV and WM hyperintensity volume has consistently been reported in the literature (Henskens et al., 2008), and our study also confirmed this association ($r=0.68$, $P<0.001$). Furthermore, our data adds to the literature by demonstrating the independent association of higher cfPWV with lower FA and higher RD in the global and regional WM fiber tracts after controlling for WM hyperintensity volume. These findings suggest an involvement of central artery stiffness in the pathogenesis of WM lesions because the lower levels of FA in the WM tissue have been shown to precede the development and progression of WM hyperintensity (de Groot et al., 2013).

Hemodynamic mechanisms underlying the association between central artery stiffness and WM lesions are likely to be multifactorial. Aortic stiffness increases left ventricular afterload and also leads to an early return of arterial wave reflections from the peripheral vascular bed (Nichols, 2005). As a result, central pulse pressure increases due to the effects of elevated forward and/or backward pressure waves (Mitchell et al., 2010; Namasivayam et al., 2009). Cerebral circulation has a high flow, low vascular resistance and impedance which may facilitate the transmission of hemodynamic pulsatility (O'Rourke and Safar,

2005). Age-related elevations in central artery stiffness and pulse pressure are independently associated with the higher levels of cerebral blood flow pulsatility and WM lesion volume (Aribisala et al., 2014; Katulska et al., 2014; Mitchell et al., 2011; Tarumi et al., 2014). Mechanistically, excessive pulsatile shear stress on cerebral microcirculations may damage vascular endothelium and blood-brain barrier whose integrity has been shown as a neuropathological correlate of WM lesions (Young et al., 2008). Therefore, central artery stiffness may increase the risk of WM lesions via elevations in central and cerebral hemodynamic pulsatility.

Central artery stiffness may also increase short-term variability in blood pressure which may predispose the brain to unstable supplies of oxygen and nutrients (Schillaci et al., 2012). In the current study, WM neuronal fiber integrity not only correlated with BRS in general, but also more closely with BRS assessed during hypotension than hypertension. Arterial baroreceptors, the stretch-sensitive mechanoreceptors located in the walls of aortic arch and carotid sinus, monitor moment-to-moment variability in arterial pressure. The baroreceptor reflex subsequently modulates cardiac output and total peripheral resistance and maintains a constant levels of systemic arterial pressure and perfusion (Lanfranchi and Somers, 2002). With stiffening of the barosensory arteries, BRS decreases and may elevate the risk of cerebral hypoperfusion in the face of hypotension (e.g., orthostasis) (Ogoh et al., 2010). Alternatively, attenuated increases in cardiac output that are accompanied by compensatory elevations in total peripheral resistance may also cause hypoperfusion, independent of arterial pressure (Guo et al., 2006). It has been shown that attenuated elevations in cardiac output during orthostasis correlate with cerebral hypoperfusion and cognitive impairment in heart failure patients (Fraser, 2014). Therefore, these findings suggest that cardiovascular regulation of arterial pressure and perfusion, especially during hypotension, may have significant impact on the structural integrity of the brain WM.

The lower levels of FA associated with arterial stiffening and decreasing BRS occurred with concurrent elevations in RD in many brain regions (Figures 1 and 2). DTI measures water diffusions in a WM fiber tract that are restricted by axonal membranes and myelin (Mori and Zhang, 2006). While FA provides an overall measure of WM neuronal fiber integrity, changes in RD, as measured by water diffusions perpendicular to the WM fiber tract, are likely to reflect myelin integrity. A series of histological experiments using the optic nerve exposed to retinal ischemia demonstrated that axonal demyelination is correlated with elevations in RD (Song et al., 2003; Sun et al., 2006). Therefore, findings from the present study suggest that cerebral hypoperfusion and/or ischemia associated with low BRS during hypotension may lead to myelin deterioration and manifest as reductions in WM FA.

The role of WM neuronal fiber integrity in cognitive function

Better executive function performance was correlated with higher FA and lower RD measured from the global and regional WM fiber tracts. The brain WM, which accounts for 40%-50% of the parenchyma, comprises axons and myelin, connects distributed network of neurons, and facilitates complex cognitive task via structural and functional integrations (Mesulam, 1990). The conventional techniques of brain WM imaging (e.g., T1-weighted or FLAIR MRI) are limited by their sensitivity in detecting changes in cognitive function. In

contrast, the diffusion metrics derived from DTI have consistently been shown to correlate with processing speed and executive function (Charlton et al., 2006). For example, Vernooij et al. reported that higher FA measured from the global WM was related to better performance on tasks assessing information processing speed and global cognition (Vernooij et al., 2009). In this regard, our data also showed that higher FA and lower RD in the global WM correlated with better executive function performance, while total brain volume of WM or WM hyperintensities were unrelated to cognitive performance.

WM neuronal fiber integrity, as assessed by FA and RD, correlated with executive function performance in all subjects. However, MCI subjects who have shown lower performance in executive function demonstrated similar levels of WM neuronal fiber integrity compared with healthy subjects. Such discrepancies in the results of group comparison versus association analyses may be explained by a few reasons. First, cognitive impairment has multifactorial causes, including but not only limited to brain WM deteriorations. The other potential causes include amyloid depositions, hypometabolism, and neurodegeneration, which may impact cognitive function independent of brain WM structural abnormalities (Arnaiz et al., 2001; Jack et al., 2009). Second, a recent meta-analysis suggested that the effect of MCI or Alzheimer disease on WM microstructural integrity may depend on the level of global cognitive impairment (e.g., MMSE) (Sexton et al., 2011). Indeed, we also observed a trend towards a positive relation between MMSE scores and global FA and RD (Data Supplement Figure). In the current study, MCI participants as a group demonstrated the comparable MMSE scores to healthy adults which in turn may have reflected the similar levels in FA and RD. Third, the metrics derived from DTI may not be specific and/or sensitive enough to detect the group difference in executive function. Finally, our study sample was relatively small and may be underpowered to detect group differences in the DTI metrics.

Strengths and Limitations

The major strength of this study is the multidisciplinary nature of the investigation. DTI assessed microstructural tissue properties of brain WM, while baroreflex-mediated control of systemic arterial perfusion was assessed by the modified Oxford technique which is currently considered the gold-standard method to quantify BRS (Lipman et al., 2003). In addition, DTI quantifies a continuous scale of WM structural characteristics as opposed to the conventional FLAIR-MRI, which only provides a dichotomous classification of normal or abnormal WM tissues. Furthermore, our sample was enriched by heterogeneous levels of cognitive function. Since MCI is a common condition in older adults, understanding the physiological link between cardiovascular and cognitive health in this population may help with the development of strategies to prevent dementia later in life.

There are several limitations that need to be discussed. First, the baroreflex pathway involves neural circuits in the brainstem which may confound an interpretation of the association between BRS and WM neuronal fiber integrity (Benarroch, 2008). Indeed, we saw that BRS was associated with FA and RD of the brainstem where the cardiovascular regulatory center is located (Figure 1). However, a stronger correlation between WM neuronal fiber integrity and BRS assessed during hypotension than hypertension and the

presence of the correlations in many other brain regions which may not relate to the baroreflex pathway make an argument that impairment in the BRS neural pathway alone cannot explain our observations. Second, anatomical orientation of the WM fiber tracts (e.g., crossing fibers and diameter of axons) may alter the level of diffusion metrics independent of the fiber integrity (Beaulieu and Allen, 1994). In this regard, TBSS may reduce such errors by analyzing the center of WM tracts common to all subjects. Third, our sample size was limited, and multiple statistical analyses were conducted, which tends to inflate Type II error. Finally, our MCI group was comprised of very mildly impaired subjects, and may not be generalizable to other populations. We did not have longitudinal data to confirm the stability or progression of MCI symptoms, and the collection of data were spread out over ~3 months, which may further attenuate relationships of interest.

Conclusions

Central artery stiffness and depressed BRS are independently associated with deterioration of WM neuronal fiber integrity in older adults. In particular, the BRS assessed during hypotension is strongly correlated with WM neuronal fiber integrity. These alterations in WM neuronal fiber are likely to be related to axonal demyelination. Finally, executive function performance is associated with WM neuronal fiber integrity, in the areas correlated with arterial stiffness and BRS. Therefore, these findings collectively suggest that cardiovascular dysregulation of systemic arterial perfusion may elevate the risk of brain WM lesions and cognitive impairment in older adults.

Supplementary Material

Refer to Web version on PubMed Central for supplementary material.

Acknowledgements

This study was supported by National Institute of Health (R01AG033106, R01HL102457, and P30AG012300) and American Heart Association (14POST20140013). The authors would like to thank the study participants for their time and effort; Yoshiyuki Okada for technical support; and Mauricio Nunez for subject recruitment effort.

References

1. Aribisala BS, Morris Z, Eadie E, Thomas A, Gow A, Hernández MCV, Royle NA, Bastin ME, Starr J, Deary IJ. Blood Pressure, Internal Carotid Artery Flow Parameters, and Age-Related White Matter Hyperintensities. Hypertension. 2014; 63:1011–1018. [PubMed: 24470459]
2. Arnaiz E, Jelic V, Almkvist O, Wahlund L, Winblad B, Valind S, Nordberg A. Impaired cerebral glucose metabolism and cognitive functioning predict deterioration in mild cognitive impairment. Neuroreport. 2001; 12:851–855. [PubMed: 11277595]
3. Beaulieu C, Allen PS. Determinants of anisotropic water diffusion in nerves. Magnetic resonance in medicine. 1994; 31:394–400. [PubMed: 8208115]
4. Benarroch EE. The arterial baroreflex Functional organization and involvement in neurologic disease. Neurology. 2008; 71:1733–1738. [PubMed: 19015490]
5. Charlton R, Barrick T, McIntyre D, Shen Y, O'Sullivan M, Howe F, Clark C, Morris R, Markus H. White matter damage on diffusion tensor imaging correlates with age-related cognitive decline. Neurology. 2006; 66:217–222. [PubMed: 16434657]
6. Cotman CW, Berchtold NC, Christie L-A. Exercise builds brain health: key roles of growth factor cascades and inflammation. Trends in neurosciences. 2007; 30:464–472. [PubMed: 17765329]

7. de Groot M, Verhaaren BF, de Boer R, Klein S, Hofman A, van der Lugt A, Ikram MA, Niessen WJ, Vernooij MW. Changes in normal-appearing white matter precede development of white matter lesions. Stroke. 2013; 44:1037–1042. [PubMed: 23429507]
8. Delis, DC.; Kramer, JH.; Kaplan, E.; Ober, BA. CVLT-II: California Verbal Learning Test Second Edition Adult Version. The Psychological Corporation; San Antonio, TX: 2000.
9. Drane DL, Yuspeh RL, Huthwaite JS, Klingler LK. Demographic characteristics and normative observations for derived-trail making test indices. Neuropsychiatry Neuropsychol Behav Neurol. 2002; 15:39–43. [PubMed: 11877550]
10. Fernando MS, Simpson JE, Matthews F, Brayne C, Lewis CE, Barber R, Kalaria RN, Forster G, Esteves F, Wharton SB, Shaw PJ, O'Brien JT, Ince PG, Function MRCC, Ageing Neuropathology Study, G. White matter lesions in an unselected cohort of the elderly: molecular pathology suggests origin from chronic hypoperfusion injury. Stroke. 2006; 37:1391–1398. [PubMed: 16627790]
11. Folstein MF, Folstein SE, McHugh PR. "Mini-mental state". A practical method for grading the cognitive state of patients for the clinician. J Psychiatr Res. 1975; 12:189–198. [PubMed: 1202204]
12. Fraser KS, Heckman GA, McKelvie RS, Harkness K, Middleton L, Hughson RL. Cerebral hypoperfusion is exaggerated with an upright posture in heart failure: impact of depressed cardiac output. JACC: Heart Failure. 2014 In Press.
13. Gauthier S, Reisberg B, Zaudig M, Petersen RC, Ritchie K, Broich K, Belleville S, Brodaty H, Bennett D, Chertkow H. Mild cognitive impairment. The Lancet. 2006; 367:1262–1270.
14. Grundman M, Petersen RC, Ferris SH, Thomas RG, Aisen PS, Bennett DA, Foster NL, Jack CR Jr. Galasko DR, Doody R, Kaye J, Sano M, Mohs R, Gauthier S, Kim HT, Jin S, Schultz AN, Schafer K, Mulnard R, van Dyck CH, Mintzer J, Zamrini EY, Cahn-Weiner D, Thal LJ. Mild cognitive impairment can be distinguished from Alzheimer disease and normal aging for clinical trials. Arch Neurol. 2004; 61:59–66. [PubMed: 14732621]
15. Guo H, Tierney N, Schaller F, Raven PB, Smith SA, Shi X. Cerebral autoregulation is preserved during orthostatic stress superimposed with systemic hypotension. Journal of Applied Physiology. 2006; 100:1785–1792. [PubMed: 16424075]
16. Gurol M, Irizarry M, Smith E, Raju S, Diaz-Arrastia R, Bottiglieri T, Rosand J, Growdon J, Greenberg S. Plasma β-amyloid and white matter lesions in AD, MCI, and cerebral amyloid angiopathy. Neurology. 2006; 66:23–29. [PubMed: 16401840]
17. Henskens LH, Kroon AA, van Oostenbrugge RJ, Gronenschild EH, Fuss-Lejeune MM, Hofman PA, Lodder J, de Leeuw PW. Increased aortic pulse wave velocity is associated with silent cerebral small-vessel disease in hypertensive patients. Hypertension. 2008; 52:1120–1126. [PubMed: 18852384]
18. Jack CR, Lowe VJ, Weigand SD, Wiste HJ, Senjem ML, Knopman DS, Shiung MM, Gunter JL, Boeve BF, Kemp BJ. Serial PIB and MRI in normal, mild cognitive impairment and Alzheimer's disease: implications for sequence of pathological events in Alzheimer's disease. Brain. 2009 awp062.
19. Jack CR Jr, Knopman DS, Jagust WJ, Petersen RC, Weiner MW, Aisen PS, Shaw LM, Vemuri P, Wiste HJ, Weigand SD. Tracking pathophysiological processes in Alzheimer's disease: an updated hypothetical model of dynamic biomarkers. The Lancet Neurology. 2013; 12:207–216. [PubMed: 23332364]
20. Katulska K, Wykrętowicz M, Minczykowski A, Krauze T, Milewska A, Piskorski J, Marciniak R, Stajgis M, Wysocki H, Guzik P. Aortic excess pressure and arterial stiffness in subjects with subclinical white matter lesions. International journal of cardiology. 2014; 172:269–270. [PubMed: 24447742]
21. Kivipelto M, Helkala E-L, Laakso MP, Hänninen T, Hallikainen M, Alhainen K, Soininen H, Tuomilehto J, Nissinen A. Midlife vascular risk factors and Alzheimer's disease in later life: longitudinal, population based study. Bmj. 2001; 322:1447–1451. [PubMed: 11408299]
22. Koepchen H. History of studies and concepts of blood pressure waves. Mechanisms of blood pressure waves. 1984:3–23.

23. Lanfranchi PA, Somers VK. Arterial baroreflex function and cardiovascular variability: interactions and implications. American Journal of Physiology-Regulatory, Integrative and Comparative Physiology. 2002; 283:R815–R826.
24. Lipman RD, Salisbury JK, Taylor JA. Spontaneous indices are inconsistent with arterial baroreflex gain. Hypertension. 2003; 42:481–487. [PubMed: 12975383]
25. Longstreth W, Manolio TA, Arnold A, Burke GL, Bryan N, Jungreis CA, Enright PL, O'Leary D, Fried L. Clinical correlates of white matter findings on cranial magnetic resonance imaging of 3301 elderly people The Cardiovascular Health Study. Stroke. 1996; 27:1274–1282. [PubMed: 8711786]
26. Madden DJ, Bennett IJ, Song AW. Cerebral white matter integrity and cognitive aging: contributions from diffusion tensor imaging. Neuropsychology review. 2009; 19:415–435. [PubMed: 19705281]
27. Maillard P, Fletcher E, Lockhart SN, Roach AE, Reed B, Mungas D, DeCarli C, Carmichael OT. White matter hyperintensities and their penumbra lie along a continuum of injury in the aging brain. Stroke. 2014; 45:1721–1726. [PubMed: 24781079]
28. Mesulam M. Large - scale neurocognitive networks and distributed processing for attention, language, and memory. Annals of neurology. 1990; 28:597–613. [PubMed: 2260847]
29. Mitchell GF, van Buchem MA, Sigurdsson S, Gotal JD, Jonsdottir MK, Kjartansson ó. Garcia M, Aspelund T, Harris TB, Gudnason V. Arterial stiffness, pressure and flow pulsatility and brain structure and function: the Age, Gene/Environment Susceptibility–Reykjavik study. Brain. 2011; 134:3398–3407. [PubMed: 22075523]
30. Mitchell GF, Wang N, Palmisano JN, Larson MG, Hamburg NM, Vita JA, Levy D, Benjamin EJ, Vasan RS. Hemodynamic correlates of blood pressure across the adult age spectrum noninvasive evaluation in the Framingham Heart Study. Circulation. 2010; 122:1379–1386. [PubMed: 20855656]
31. Monahan KD, Tanaka H, Dinenno FA, Seals DR. Central arterial compliance is associated with age-and habitual exercise–related differences in cardiovagal baroreflex sensitivity. Circulation. 2001; 104:1627–1632. [PubMed: 11581140]
32. Moody DM, Bell MA, Challa VR. Features of the cerebral vascular pattern that predict vulnerability to perfusion or oxygenation deficiency: an anatomic study. AJNR Am J Neuroradiol. 1990; 11:431–439. [PubMed: 2112304]
33. Mori S, Oishi K, Jiang H, Jiang L, Li X, Akhter K, Hua K, Faria AV, Mahmood A, Woods R. Stereotaxic white matter atlas based on diffusion tensor imaging in an ICBM template. Neuroimage. 2008; 40:570–582. [PubMed: 18255316]
34. Mori S, Zhang J. Principles of diffusion tensor imaging and its applications to basic neuroscience research. Neuron. 2006; 51:527–539. [PubMed: 16950152]
35. Morris JC, Ernesto C, Schafer K, Coats M, Leon S, Sano M, Thal LJ, Woodbury P. Clinical dementia rating training and reliability in multicenter studies: the Alzheimer's Disease Cooperative Study experience. Neurology. 1997; 48:1508–1510. [PubMed: 9191756]
36. Namasivayam M, McDonnell BJ, McEniery CM, O'Rourke MF. Does wave reflection dominate age-related change in aortic blood pressure across the human life span? Hypertension. 2009; 53:979–985. [PubMed: 19380614]
37. Nichols, WW.; O'Rourke, ME. McDonald's Blood Flow in Arteries. 5th ed. Oxford University Press; New York: 2005.
38. O'Rourke MF, Safar ME. Relationship between aortic stiffening and microvascular disease in brain and kidney: cause and logic of therapy. Hypertension. 2005; 46:200–204. [PubMed: 15911742]
39. Ogoh S, Tzeng Y-C, Lucas SJ, Galvin SD, Ainslie PN. Influence of baroreflex-mediated tachycardia on the regulation of dynamic cerebral perfusion during acute hypotension in humans. The Journal of physiology. 2010; 588:365–371. [PubMed: 19933752]
40. Petersen RC, Doody R, Kurz A, Mohs RC, Morris JC, Rabins PV, Ritchie K, Rossor M, Thal L, Winblad B. Current concepts in mild cognitive impairment. Archives of neurology. 2001; 58:1985–1992. [PubMed: 11735772]

41. Petersen RC, Smith GE, Waring SC, Ivnik RJ, Tangalos EG, Kokmen E. Mild cognitive impairment: clinical characterization and outcome. Archives of neurology. 1999; 56:303–308. [PubMed: 10190820]
42. Rothwell PM. Limitations of the usual blood-pressure hypothesis and importance of variability, instability, and episodic hypertension. The Lancet. 2010; 375:938–948.
43. Rothwell PM, Howard SC, Dolan E, O'Brien E, Dobson JE, Dahlöf B, Sever PS, Poulter NR. Prognostic significance of visit-to-visit variability, maximum systolic blood pressure, and episodic hypertension. The Lancet. 2010; 375:895–905.
44. Rudas L, Crossman AA, Morillo CA, Halliwill JR, Tahvanainen KU, Kuusela TA, Eckberg DL. Human sympathetic and vagal baroreflex responses to sequential nitroprusside and phenylephrine. American Journal of Physiology-Heart and Circulatory Physiology. 1999; 276:H1691–H1698.
45. Rueckert D, Sonoda LI, Hayes C, Hill DL, Leach MO, Hawkes DJ. Nonrigid registration using free-form deformations: application to breast MR images. Medical Imaging, IEEE Transactions on 18. 1999:712–721.
46. Rusanen M, Kivipelto M, Levälahti E, Laatikainen T, Tuomilehto J, Soininen H, Ngandu T. Heart Diseases and Long-Term Risk of Dementia and Alzheimer's Disease: A Population-Based CAIDE Study. Journal of Alzheimer's Disease. 2014
47. Schillaci G, Bilo G, Pucci G, Laurent S, Macquin-Mavier I, Boutouyrie P, Battista F, Settimi L, Desamericq G, Dolbeau G. Relationship between short-term blood pressure variability and large-artery stiffness in human hypertension findings from 2 large databases. Hypertension. 2012; 60:369–377. [PubMed: 22753222]
48. Sexton CE, Kalu UG, Filippini N, Mackay CE, Ebmeier KP. A meta-analysis of diffusion tensor imaging in mild cognitive impairment and Alzheimer's disease. Neurobiology of aging. 2011; 32:2322, e2325–2322, e2318. [PubMed: 20619504]
49. Smith SM. Fast robust automated brain extraction. Human brain mapping. 2002; 17:143–155. [PubMed: 12391568]
50. Smith SM, Jenkinson M, Johansen-Berg H, Rueckert D, Nichols TE, Mackay CE, Watkins KE, Ciccarelli O, Cader MZ, Matthews PM. Tract-based spatial statistics: voxelwise analysis of multi-subject diffusion data. Neuroimage. 2006; 31:1487–1505. [PubMed: 16624579]
51. Smith SM, Jenkinson M, Woolrich MW, Beckmann CF, Behrens TE, Johansen-Berg H, Bannister PR, De Luca M, Drobnjak I, Flitney DE. Advances in functional and structural MR image analysis and implementation as FSL. Neuroimage. 2004; 23:S208–S219. [PubMed: 15501092]
52. Song S-K, Sun S-W, Ju W-K, Lin S-J, Cross AH, Neufeld AH. Diffusion tensor imaging detects and differentiates axon and myelin degeneration in mouse optic nerve after retinal ischemia. Neuroimage. 2003; 20:1714–1722. [PubMed: 14642481]
53. Sun S-W, Liang H-F, Le TQ, Armstrong RC, Cross AH, Song S-K. Differential sensitivity of in vivo and ex vivo diffusion tensor imaging to evolving optic nerve injury in mice with retinal ischemia. Neuroimage. 2006; 32:1195–1204. [PubMed: 16797189]
54. Tanaka H, Dinenno FA, Monahan KD, Clevenger CM, DeSouza CA, Seals DR. Aging, habitual exercise, and dynamic arterial compliance. Circulation. 2000; 102:1270–1275. [PubMed: 10982542]
55. Tarumi T, Khan MA, Liu J, Tseng BM, Parker R, Riley J, Tinajero C, Zhang R. Cerebral hemodynamics in normal aging: central artery stiffness, wave reflection, and pressure pulsatility. Journal of Cerebral Blood Flow & Metabolism. 2014
56. Tombaugh TN. Trail Making Test A and B: normative data stratified by age and education. Arch Clin Neuropsychol. 2004; 19:203–214. [PubMed: 15010086]
57. Tsao CW, Seshadri S, Beiser AS, Westwood AJ, Decarli C, Au R, Himali JJ, Hamburg NM, Vita JA, Levy D, Larson MG, Benjamin EJ, Wolf PA, Vasan RS, Mitchell GF. Relations of arterial stiffness and endothelial function to brain aging in the community. Neurology. 2013; 81:984–991. [PubMed: 23935179]
58. Vernooij MW, Ikram MA, Vrooman HA, Wielopolski PA, Krestin GP, Hofman A, Niessen WJ, Van der Lugt A, Breteler MM. White matter microstructural integrity and cognitive function in a general elderly population. Archives of General Psychiatry. 2009; 66:545–553. [PubMed: 19414714]

59. Wardlaw JM, Smith EE, Biessels GJ, Cordonnier C, Fazekas F, Frayne R, Lindley RI, O'Brien JT, Barkhof F, Benavente OR. Neuroimaging standards for research into small vessel disease and its contribution to ageing and neurodegeneration. The Lancet Neurology. 2013; 12:822–838. [PubMed: 23867200]

60. Wechsler, D. Wechsler Memory Scale-Revised. Psychological Corp; New York: 1987.

61. Wentzel C, Rockwood K, MacKnight C, Hachinski V, Hogan D, Feldman H, Østbye T, Wolfson C, Gauthier S, Verreault R. Progression of impairment in patients with vascular cognitive impairment without dementia. Neurology. 2001; 57:714–716. [PubMed: 11524488]

62. Young VG, Halliday GM, Kril JJ. Neuropathologic correlates of white matter hyperintensities. Neurology. 2008; 71:804–811. [PubMed: 18685136]

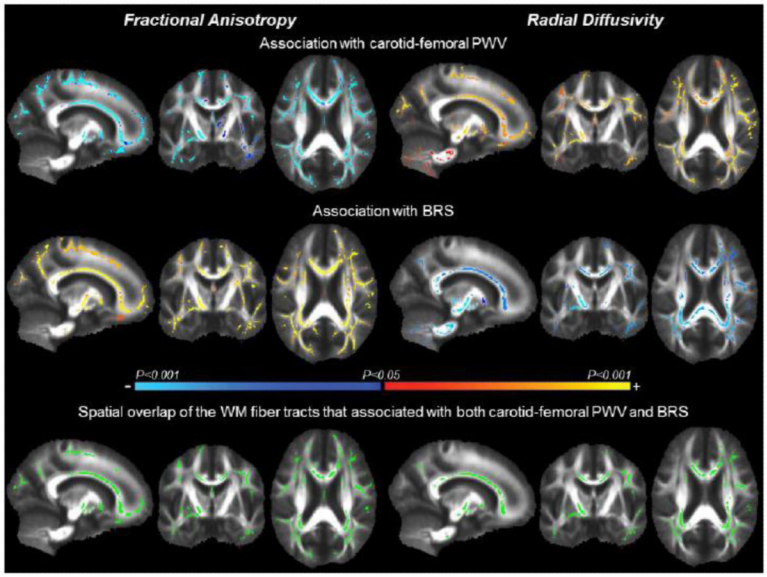

Figure 1.

Tract-based spatial statistic (TBSS) maps exhibit white matter (WM) fiber tracts with fractional anisotropy (left) and radial diffusivity (right) that associated with carotid-femoral pulse wave velocity (PWV) (top) and baroreflex sensitivity (BRS) (middle). The color bar illustrates the directionality and *P-value* of the associations. The bottom images show spatial overlap of the WM fiber tracts (green) that associated with both carotid-femoral PWV and BRS.

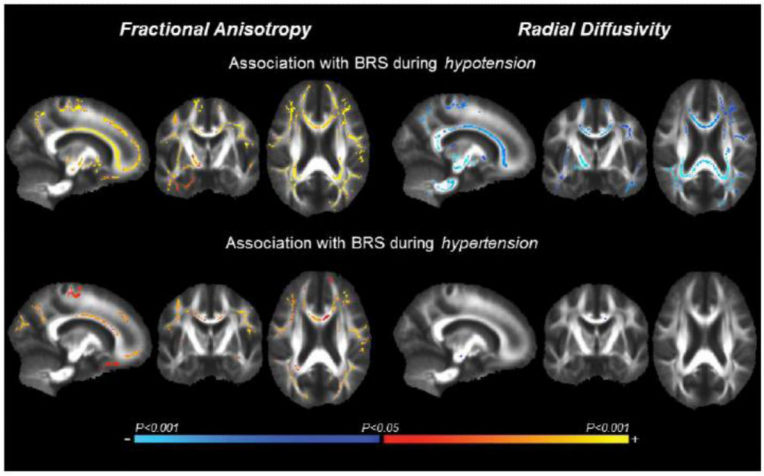

Figure 2.

Tract-based spatial statistic (TBSS) maps exhibit white matter fiber tracts with fractional anisotropy (left) and radial diffusivity (right) that associated with baroreflex sensitivity (BRS), as assessed separately during hypotension (top) and hypertension (bottom). The color bar illustrates the directionality and *P-value* of the associations.

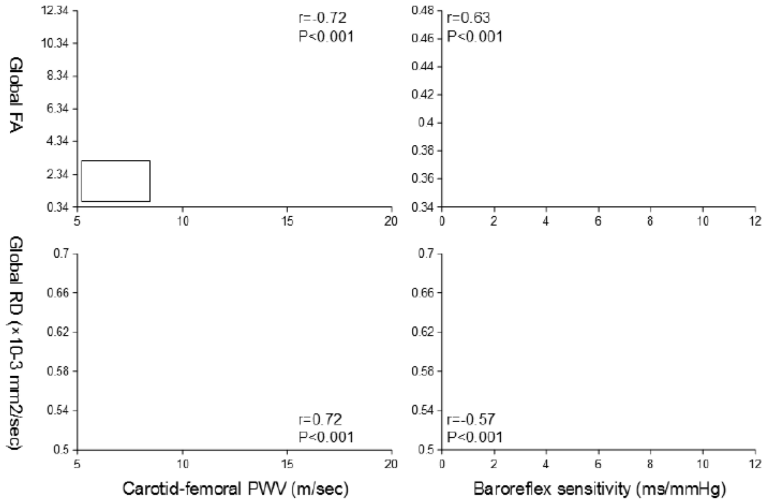

Figure 3.

Scatter plots show simple correlations of carotid-femoral pulse wave velocity (PWV) (left) and baroreflex sensitivity (right) with fractional anisotropy (FA) (top) and radial diffusivity (RD) (bottom). Mean values of FA and RD were extracted from the global WM skeleton that associated with both carotid-femoral PWV and baroreflex sensitivity (see the bottom of Figure 1).

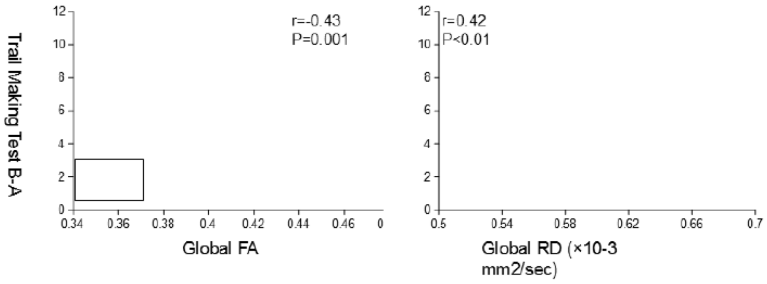

Figure 4.

Scatter plots show simple correlations of fractional anisotropy (FA) (left) and radial diffusivity (RD) (right) with the scores from the Trail Making Test B-A index. Mean values of FA and RD were extracted from the global WM skeleton that associated with both carotidfemoral PWV and baroreflex sensitivity (see the bottom of Figure 1).

Table 1

Sample characteristics of all, cognitively normal, and MCI subjects

	All	Normal	MCI	*P-value*
Men/Women (n)	26/28	10/8	16/20	0.44
Age (years)	65 ± 6	65 ± 6	66 ± 7	0.59
Education (years)	16 ± 2	17 ± 2	16 ± 2	0.29
Height (cm)	170 ± 8	171 ± 9	170 ± 8	0.64
Body mass (kg)	80 ± 14	80 ± 16	80 ± 13	0.89
Body mass index (kg/m^2)	27 ± 4	27 ± 4	28 ± 4	0.50
Neurocognitive measures				
Mini-Mental State Exam	29 ± 1	29 ± 1	29 ± 1	0.46
CVLT Short Delay Free Recall	10 ± 3	11 ± 2	9 ± 2	**<0.01**
CVLT Long Delay Free Recall	10 ± 3	12 ± 2	10 ± 3	**<0.01**
Trail Making Test part A	28 ± 10	29 ± 11	27 ± 9	0.80
Trail Making Test part B	72 ± 25	62 ± 18	77 ± 26	**0.01**
Trail Making Test part B-A	44 ± 21	33 ± 16	49 ± 21	**<0.01**
Cardiovascular measures				
Systolic BP (mmHg)	124 ± 14	125 ± 14	124 ± 14	0.82
Diastolic BP (mmHg)	74 ± 8	74 ± 9	74 ± 8	0.82
Heart rate (bpm)	61 ± 10	63 ± 10	60 ± 11	0.34
Carotid-femoral PWV (m/sec)	11.0 ± 2.7	11.2 ± 2.2	11.0 ± 2.9	0.54
BRS (ms/mmHg)	4.99 ± 2.33	5.09 ± 2.80	4.94 ± 2.10	0.91
Brain volumetric measures				
Total grey matter volume (%ICV)	39.7 ± 2.4	40.3 ± 2.1	39.4 ± 2.6	0.23
Total white matter volume (%ICV)	34.7 ± 3.1	34.7 ± 2.3	34.7 ± 3.5	0.83
Medial temporal lobe volume (%TB)	1.62 ± 0.13	1.63 ± 0.13	1.62 ± 0.12	0.73
Hippocampus volume (%TB)	0.69 ± 0.08	0.69 ± 0.06	0.69 ± 0.09	0.93
Total WMH volume (%ICV)	0.27 ± 0.44	0.25 ± 0.39	0.29 ± 0.46	0.79

Bold: P-value<0.05 between normal vs. MCI subjects. Values are mean ± standard deviation. BP=blood pressure, BRS=baroreflex sensitivity, CVLT=California Verbal Learning Test, ICV=intracranial volume, MCI=mild cognitive impairment, PWV=pulse wave velocity, TB=total brain volume, and WMH=white matter hyperintensity. %ICV and %TB represent brain volume normalized to intracranial and total brain volumes respectively.

Table 2

Multivariate adjusted relations of central artery stiffness and baroreflex sensitivity with microstructural tissue integrity of global and regional white matter fiber tracts, as assessed by fractional anisotropy

White matter regions		Carotid-femoral PWV		Baroreflex sensitivity	
		β ± SE	*P-value*	β ± SE	P-value
Global white matter		−0.37 ± 0.11	**<0.01**	0.39 ± 0.10	**<0.001**
Corpus callosum	genu	−0.29 ± 0.18	0.12	0.15 ± 0.15	0.32
	body	−0.90 ± 0.17	0.59	0.03 ± 0.14	0.86
	splenium	−0.32 ± 0.19	0.10	0.32 ± 0.16	**0.049**
Corona radiata	anterior	−0.13 ± 0.16	0.40	0.12 ± 0.13	0.37
	superior	−0.25 ± 0.19	0.20	0.20 ± 0.16	0.23
	posterior	−0.46 ± 0.15	**<0.01**	0.40 ± 0.13	**<0.01**
Internal capsule	anterior limb	−0.26 ± 0.15	0.10	0.14 ± 0.13	0.29
	posterior limb	−0.27 ± 0.14	0.07	0.06 ± 0.12	0.63
	retrolenticular part	−0.34 ± 0.18	0.06	0.32 ± 0.15	**0.04**
External capsule		−0.19 ± 0.16	0.25	0.27 ± 0.14	0.053
Superior longitudinal fasciculus		−0.32 ± 0.18	0.09	0.25 ± 0.15	0.10

Bold: P-value<0.05. The mean values of fractional anisotropy were extracted from the global and regional white matter fiber tracts that associated with both carotid-femoral PWV and baroreflex sensitivity (see the bottom left of Figure 1). All models adjusted for age, sex, education level, systolic blood pressure, and total brain volume of white matter hyperintensity. Total brain volume of white matter hyperintensity was log-transformed before entered in the model. β=standardized regression coefficient, PWV=pulse wave velocity, and SE=standard error

Table 3

Multivariate adjusted relations of central artery stiffness and baroreflex sensitivity with microstructural tissue integrity of global and regional white matter fiber tracts, as assessed by radial diffusivity

White matter regions		Carotid-femoral PWV		Baroreflex sensitivity	
		β ± SE	*P-value*	β ± SE	*P-value*
Global white matter		0.38 ± 0.12	**<0.01**	−0.39 ± 0.10	**0.001**
Corpus callosum	genu	0.32 ± 0.17	0.07	−0.24 ± 0.14	0.10
	body	0.31 ± 0.16	0.055	−0.12 ± 0.13	0.37
	splenium	0.36 ± 0.18	0.055	−0.39 ± 0.15	**0.01**
Corona radiata	anterior	0.30 ± 0.14	**0.03**	−0.30 ± 0.11	**0.01**
	superior	0.28 ± 0.15	0.07	−0.28 ± 0.13	**0.04**
	posterior	0.47 ± 0.15	**<0.01**	−0.32 ± 0.12	**0.01**
Internal capsule	anterior limb	0.18 ± 0.17	0.29	−0.16 ± 0.14	0.25
	posterior limb	0.24 ± 0.16	0.14	−0.04 ± 0.13	0.78
	retrolenticular part	0.37 ± 0.17	**0.03**	−0.28 ± 0.14	**0.047**
External capsule		0.29 ± 0.16	0.07	−0.24 ± 0.13	0.08
Superior longitudinal fasciculus		0.38 ± 0.17	**0.04**	−0.23 ± 0.15	0.13

Bold: P-value<0.05. The mean values of radial diffusivity were extracted from the global and regional white matter fiber tracts that associated with both carotid-femoral PWV and baroreflex sensitivity (see the bottom right of Figure 1). All models adjusted for age, sex, education level, systolic blood pressure, and total brain volume of white matter hyperintensity. Total brain volume of white matter hyperintensity was log-transformed before entered in the model. β=standardized regression coefficient, PWV=pulse wave velocity, and SE=standard error